SN 1999ac: On the presence of high velocity carbon.

G. Garavini[1], G. Aldering[2,3], R. Amanullah[1], P. Astier[4], C. Balland[4,5], G. Blanc[2], M. S. Burns[6], A. Conley[2,7], T. Dahlén[8], S. E. Deustua[2,9], R. Ellis[10], S. Fabbro[11], X. Fan[12], G. Folatelli[1], B. Frye[2], E. L. Gates[13], R. Gibbons[2], G. Goldhaber[2,7], B. Goldman[14], A. Goobar[1], D. E. Groom[2], D. Hardin[4], I. Hook[15], D. A. Howell[2], D. Kasen[2], S. Kent[16], A. G. Kim[2], R. A. Knop[17], B. C. Lee[2], C. Lidman[18], J. Mendez[19,20], G. Miller, M. Moniez[21], M. Mouchet[22], A. Mourão[11], H. Newberg[23], S. Nobili[1], P. E. Nugent[2], R. Pain[4], N. Panagia[24], O. Perdereau[21], S. Perlmutter[2], V. Prasad[2], R. Quimby[2], J. Raux[4], N. Regnault[2], J. Rich[25], G. T. Richards [26], P. Ruiz-Lapuente[20], G. Sainton[4], B. Schaefer[27], K. Schahmaneche[4], E. Smith[17], A. L. Spadafora[2], V. Stanishev[1], N. A. Walton[28], L. Wang[2], W. M. Wood-Vasey[2,7], N. Yasuda[29], T. York[2], (THE SUPERNOVA COSMOLOGY PROJECT).

[1]Department of Physics, Stockholm University, Albanova University Center, S-106 91 Stockholm, Sweden

[2]E. O. Lawrence Berkeley National Laboratory, 1 Cyclotron Rd., Berkeley, CA 94720, USA

[3]Visiting Astronomer, Cerro Tololo Interamerican Observatory, National Optical Astronomy Observatory, which is operated by the Association of Universities for Research in Astronomy, Inc. (AURA) under cooperative agreement with the National Science Foundation.

[4]LPNHE, CNRS-IN2P3, University of Paris VI & VII, Paris, France

[5]Université Paris Sud, IAS-CNRS, Bâtiment 121, 91405 Orsay Cedex, France

[6]Colorado College 14 East Cache La Poudre St., Colorado Springs, CO 80903

[7]Department of Physics, University of California Berkeley, Berkeley, 94720-7300 CA, USA

[8]Stockholm Observatory, Albanova University Center, S-106 91 Stockholm, Sweden

[9]American Astronomical Society, 2000 Florida Ave, NW, Suite 400, Washington, DC, 20009 USA.

[10]California Institute of Technology, E. California Blvd, Pasadena, CA 91125, USA

[11]CENTRA-Centro M. de Astrofísica and Department of Physics, IST, Lisbon, Portugal

[12]Steward Observatory, the University of Arizona, Tucson , AZ 85721

[13]Lick Observatory, P.O. Box 85, Mount Hamilton, CA 95140

[14]Department of Astronomy, New Mexico State University, Dept. 4500, P.O. Box 30001, Las Cruces, NM 88011

[15]Department of Physics, University of Oxford, Nuclear & Astrophysics Laboratory Keble Road, Oxford, OX1 3RH, UK

[16]Fermi National Accelerator Laboratory, P.O. Box 500, Batavia, IL 60510

[17]Department of Physics and Astronomy, Vanderbilt University, Nashville, TN 37240, USA

[18]European Southern Observatory, Alonso de C ordova 3107, Vitacura, Casilla 19001,

Santiago 19, Chile

[19]Isaac Newton Group, Apartado de Correos 321, 38780 Santa Cruz de La Palma, Islas Canarias, Spain

[20]Department of Astronomy, University of Barcelona, Barcelona, Spain

[21]Laboratoire de l'Accélerateur Linéaire, IN2P3-CNRS, Université Paris Sud, B.P. 34, 91898 Orsay Cedex, France

[22]LUTH Observatoire de Paris, Section de Meudon, 92195 Meudon Cedex, France

[23]Rensselaer Polytechnic Institute, Physics Dept., SC1C25, Troy NY 12180, U.S.A.

[24]Space Telescope Science Institute, 3700 San Martin Drive, Baltimore, MD 21218, USA

[25]DAPNIA-SPP, CEA Saclay, 91191 Gif-sur-Yvette, France

[26]University of Chicago, Astronomy & Astrophysics Center, 5640 s. Ellis Ave., Chicago IL 60637

[27]University of Texas, Department of Astronomy, C-1400, Austin, TX,78712, U.S.A.

[28]Institute of Astronomy, Madingley Road, Cambridge CB3 0HA, UK

[29]National Astronomical Observatory, Mitaka, Tokyo 181-8588, Japan

ABSTRACT

We present an analysis of the optical spectroscopic data for the peculiar Type Ia supernova SN 1999ac. Our data set covers from day -15 to +42 with respect to B-band light curve maximum. SN 1999ac is unusual in many respects. Prior to B-band maximum, the spectra of SN 1999ac resemble a SN 1999aa-like object (slow decliner) but with stronger Si II and Ca II H&K, i.e. somewhat closer to Branch-normal supernovae. We study the atmosphere composition of the early spectra by means of SYNOW synthetic spectra. We find convincing evidence of high velocity (v>16000 km s^{-1}) carbon forming distinct C II $\lambda4743$, C II $\lambda6580$, C II $\lambda7324$ absorption features in the -15 days spectrum. At the same epoch C III $\lambda4649$ at photospheric velocity is probably responsible for a small absorption at 4500Å. Furthermore, we study the time evolution of the expansion velocity as inferred from the measurement of the Ca H&K and Si II $\lambda6355$ absorption features. We found values for Ca H&K within those seen for normal Type Ia SNe. The velocities of Si II $\lambda6355$ resemble instead the behaviour of under-luminous objects. These characteristics are unique among Type Ia supernovae and remain unexplained within the currently available models.

1. Introduction

The increasing collection of high signal-to-noise data has shown that Type Ia supernovae (SNe Ia) explosions show significant differences in their characteristics. Model predictions are compared with observations to address the question whether we can regard all Type Ia supernovae as originating from the same kind of physical phenomenon.

The most widely accepted model for Type Ia supernovae involves the thermonuclear

disruption of a C+O white dwarf star (WD) accreting material from a companion star (Whelan & Iben 1973; Nomoto 1982; Iben 1984; Paczynski 1985). The atmospheric composition produced by traditional 1D pure deflagration explosion models (such as W7, Nomoto et al. (1984)) consists of a layered structure with the inner core populated by iron-group elements (e.g: Fe Co and Ni) surrounded by a region of intermediate mass elements (IME, e.g: Si, Ca, S and Mg). The outermost layer contains the original unburned composition. Thus, absorption lines produced by C at high velocity are expected to be found in pre-maximum spectra of SNe Ia in pure deflagration models. The velocity distribution of Si, Ca, Mg, Fe, Co and Ni may differ if the supernova explosion is instead modeled as a delayed-detonation (DD models). The study of the velocity distribution of such ions in observed spectra can yield information on the dynamics of the explosion.

Recently, full 3D explosion models have been produced (Khokhlov 2000; Gamezo et al. 2003). Driven by these developments the first attempts to study 3D spectral signature have been made (Thomas et al. 2002; Baron et al. 2003; Kasen et al. 2003). In 3D explosion models convective flows allow the external material to be transported into the internal regions of the atmosphere. This presents the possibility of finding signs of the original composition at any distance from the centre and intermediate mass elements forming clumps at high velocities. For other supernovae, Kasen et al. (2003); Branch et al. (2003); Garavini et al. (2003) showed probable evidence for unburned material on a wide velocity range as well as high-velocity burned material. These findings suggest the need of 3D simulations for describing some of the observations.

Type Ia supernovae are usually classified in sub-groups according to their spectro-photometric properties as peculiar slow-decliner SN 1991T-like (Phillips et al. 1992; Ruiz-Lapuente et al. 1992), Branch-normal (Branch et al. 1983, 1993) and peculiar fast-decliner SN 1991bg-like (Filippenko 1992). Recent work has shown that the gap

in spectral characteristcs between SN 1991T-like and Branch-normal could be filled as new supernovae are discovered. The most extreme peculiar slow-decliner SNe Ia, such as SN 2000cx (Li et al. 2001a), seem now to be at one end of a sequence that has at the other end the more common normal SNe Ia. Supernovae such as SN 1999aa (Garavini et al. 2003), SN 1999aw (Strolger et al. 2003) or SN 2002cu (Li 2002), for example, share spectroscopical and photometric characteristics of both sub-groups. However, new observations are showing a variety of spectral and photometric peculiarities (see e.g. SN 2002cx Li et al. (2003) or SN 2001ay Howell et al. (2003)) that are strengthening the conviction that SNe Ia can not be described only as one parameter sequence of objects.

In this work the optical spectroscopy data of SN 1999ac collected by the Supernova Cosmology Project (SCP) collaboration during the Spring 1999 campaign (for details see Aldering (2000); Nugent & Aldering (2000)) is presented and analyzed. SN 1999ac can be classified as a SN 1999aa-like object with spectral characteristics closer to normal supernovae. The optical light curve is peculiar (Phillips et al. 2002), rising as a slow decliner object (e.g SN 1991T) and transitioning a faster decline after maximum with $\Delta m_{15}=1.30\pm0.09$ (Li et al. 2003).

In the present work we use the direct analysis code SYNOW (Fisher et al. 1997, 1999) and the measurements of velocities inferred from the minima of the spectral features to identify ions responsible for the observed features and their velocity distribution to investigate the structure of the expanding atmosphere. In particular, we have looked for evidence of carbon and hydrogen lines in early spectra and measured the velocity range of intermediate mass elements with the aim of finding possible fingerprints of the progenitor system and to help in constraining the dynamics of the explosion models.

In section 2 a description of the data set and reduction scheme is given. Section 3 presents the spectra of SN 1999ac. SYNOW synthetic spectra for the two pre-maximum

light epochs are presented in section 4. In section 5 we present the expansion velocities as _our findings is presented_ inferred from the minima of CaH&K and Si II λ6355. The discussion of ~~the results is held~~ in section 6.

2. Data Set and Reduction Method

SN 1999ac (R.A. = $16^h07^m15.0^s$ Decl. =$+07^d58'20''$, equinox 2000.0) was discovered and confirmed on unfiltered observations taken on Feb. 26.5 and 27.5 UT at 23".9 east and 29".8 south of the host galaxy nucleus (Modjaz et al. 1999). Fig. 1 shows the position of SN 1999ac in its host galaxy NGC 6063, a S(D) _Scd(?)_ with a recession velocity of 2848 km s^{-1} _This was_ determined from narrow H-alpha emission (Theureau et al. 1998).

Phillips et al. (1999) and Kiss et al. (1999) réported that the confirmation spectrum _a_ taken on Feb. 28 UT was similar to ~~the one~~ _that_ of SN 1999aa _but_ with stronger Si II λ6355 and well defined Ca H&K.

According to Schlegel et al. (1998) the galactic reddening in the direction of SN 1999ac is $E(B - V) = 0.046$ mag. The photometric characteristic makes difficult the estimate of the host galaxy reddening (Phillips et al. 2002). _what does this mean?_

The SCP carried out an extensive follow-up both spectroscopically and photometrically. In this work the spectroscopy data set is presented.

The data set consists _of_ in 13 optical spectra dating from day -15 to day $+42$ (all epochs are given with respect to the B-band maximum). In most of the cases the spectra were acquired using different instrumental settings for the blue and the red part of the spectrum in order to avoid possible second order contaminations. The 13 final spectra are then the combination of ~~both parts~~ _wavelength ranges_. The spectral time evolution is shown in Fig. 2 and the data set log is reported in table 1.

The data were reduced using standard IRAF routines. The two dimensional images were bias-subtracted and flat-fielded. The sky background was fitted, subtracted and extracted for systematics checks on the wavelength calibration. Wavelength and flux calibration were applied to the 1D extracted spectrum using calibration observations taken with the same instrumental setting and during the same night as the science observations. The accuracy of the wavelength calibration was checked against the extracted sky spectrum and generally found to agreement within 2 Å.

Atmospheric extinction correction was applied via tabulated extinction coefficients for each telescope used. A correction for the Milky Way extinction was applied (Cardelli et al. 1989) assuming $R_V = 3.1$, i.e $A_V = 0.14$. The amount of host-galaxy contamination was checked by χ^2-fitting the host galaxy spectrum contribution to the data with respect to a supernova spectral template, and found to be negligible at all epochs. Therefore no host galaxy subtraction was performed. The complete description of the data reduction method will be presented in a forthcoming work (Folatelli et al. 2003).

This is consist w/ SN 1999ac's separation from the host seen in Fig 1

additional (e.g. host was subtract along w/ sky)

3. Spectral Time Evolution

The time span of the data set allows the study of the time evolution of the spectroscopic characteristics of SN 1999ac beginning just days after the explosion and continuing through seven weeks after B-band maximum light. In Fig. 2 our spectral time sequence is shown.

The spectrum at −15 days is among the earliest available for a type Ia supernovae and shows SN 1999ac as a SN 1999aa-like object with stronger Si II $\lambda6355$ and Ca II H&K and weaker Fe III $\lambda\lambda4404$ and 5129. The spectral evolution shows Si II and Ca II lines becoming stronger, along with the development of the other typical features of Branch-normal supernovae. Si II $\lambda6355$ becomes contaminated by Fe II lines already at +11 days and by +24 days is part of a broad feature with four minima. Ca II H&K keeps a constant profile

all along the time sequence showing a single and well defined minimum. The 'W' shaped S II $\lambda\lambda$5449,5628 becomes evident only around maximum light and maintains a ~~red~~ component ~~deeper~~ than that on the blue . One week after maximum this absorption disappears and is ~~substituted~~ by Fe II and Na I lines. The Ca IR triplet (around 8000 Å) deepens with time, ~~first~~ but remains relatively constant in strength ~~from~~ about three weeks past maximum ~~onward~~. The lines of the iron group elements (Fe, Co, Ni) become increasingly prominent starting from about two weeks after maximum. At three weeks after maximum they dominate the whole spectral range from ultra-violet to the near infrared with the exception of Ca II H&K and IR triplet.

The whole spectral time evolution resembles that of normal supernovae ~~beyond maximum light~~. The more evident spectral peculiarities are in the pre-maximum spectra, thus, we compare ~~them with other supernovae~~. Fig. 3 shows the −15 days spectrum. The lines that characterize normal type Ia supernovae in pre-maximum spectra are Ca II H&K and Si II λ6355 and as already ~~noticed~~ can both be seen in SN 1999ac (even if the blue end of Ca H&K is not covered by our spectrum). SN 1999ac shows stronger Ca H&K and Si II absorptions compared to the other peculiar objects (SN 1999aa and SN 1991T) and has weaker Fe III $\lambda\lambda$4404,5129 and Si III λ4560 lines that represent the signatures of genuine SN 1991T-like objects. Two small absorptions respectively on the red side of Si II λ6355 and around 7000 Å are clearly visible, both on SN 1999ac and in SN 1990N, and are probably due to C II $\lambda\lambda$6580,7234. The spectral characteristics of SN 1999ac at this epoch position this supernova between Branch-normal and SN 1999aa-like objects.

The spectrum at day −9 is similar to the one at day −15. The comparison with normal and peculiar supernovae is shown in Fig. 4. Our spectrum does not cover the region of Ca H&K. The two Fe III lines ($\lambda\lambda$4404,5129) look still much weaker than in SN 1991T and ~~with~~ rounded minima. The contribution from Fe II in the region between 4000 and 5000 Å

appears weaker than in normal SNe. Si II $\lambda6355$ has now become broader. The absorption features present on the red edge of this line and that around 7000 Å at day -15 are no longer evident. *useful to divide −15 day by −9 day?*

In the next section we make a direct analysis of the pre-maximum light spectra to identify the observed absorption features.

Read only quickly b/c telluric not treated

4. Synthetic Spectra

We used SYNOW to produce synthetic spectra and to investigate line identifications and velocity ranges.

SYNOW generates spectra using an homologously expanding supernova envelope. This model consists of a continuum-emitting, sharply defined photosphere (approximated with a black body emission) surrounded by an extended line-forming, pure scattering atmosphere. Line transfer is treated using the Sobolev method (Sobolev 1960; Castor 1970; Jeffrey & Brach 1990) so line opacity is parameterised in terms of Sobolev optical depth. Which ions are used in the calculation is guided by experience and the SN ion signatures atlas of Hatano et al. (1999a). For each ion introduced, Sobolev optical depth as a function of radius for a "reference line" (usually a strong optical line) is specified. Optical depths in other lines of the ion are set assuming Boltzmann excitation of the levels at temperature T_{exc}.

The parameters v_{phot} and T_{bb} set the velocity and blackbody continuum temperature of the photosphere, respectively. For each ion, optical depth τ and the specified minimum, ejection velocity v_{min} is given. Optical depth scales exponentially with velocity according to e-folding velocity up to a maximum velocity given by v_{max}. If $v_{min} > v_{phot}$ for an ion, we refer to the ion as "detached."

The black body assumption is a basic simplification of the processes that contribute to form the continuum emission therefore T_{bb} can not be regarded as physical information. Thus, SYNOW produces only a rough indication of the continuum level, which can disagree with the observed spectrum. We handled this by bringing the blue portions of the observed and modelled spectra into agreement. The continuum mismatches which then occur at longer wavelengths have not adversely affected our study of the few spectral features present in the red.

We used the code to generate synthetic spectra to investigare possible line identifications and velocity ranges for the spectra at 15 and 9 days before B-band maximum light. The input parameters used in the best match spectrum provide a picture of the ions and velocity ranges producing the observed absorptions and can be used as hints for the more rigorous hydrodynamical models.

Day -15

Fig. 5 shows the SYNOW synthetic spectrum computed for -15 days using the input parameters shown in Table 2. The velocity range in which we introduce Ca II is mainly constrained by the Ca II IR triplet since the H&K component is essentially missing in our spectrum. Si II ($v_{min} = 14200$ km s^{-1}) is detached above the photosphere (v_{phot}=13000 km s^{-1}) in order to match wavelength of the minimum at 6150 Å. Si III instead requires $v_{max} = 17000$ km s^{-1} to match the line at 4400 Å. Fe III matches the profile of the two lines, (4200 Å and 4900 Å) when introduced between $v_{min} = 14500$ km s^{-1} and $v_{max} = 18000$ km s^{-1}. The weak absorption at 6300 Å is well matched by a detached C II ($v_{min} = 16000$ km s^{-1}) that also contributes to the line near 4500Å and 7000 Å. The wavelength regions were C II makes its contribution are highlighted in Fig. 6 showing the effect of this ion on the model. The good matching between the absorption feature at 6300 Å and the contribution near

4500 Å and near 7000 Å makes the identification of a high velocity C II layer plausible.

C III at photospheric velocity matches the small notch on the red edge of Si III near $\lambda 4500$ Å. The evidence for the contribution of C III to the spectrum is less convincing than that of C II. Fig. 7 shows the comparison between the data and different models in the 4500 Å region. To understand the impact of C III on the matching, models with and without C III and C II are shown. The small absorption at 4500 Å can be reproduced with C III that, however, does not form any other line. The mismatch found when C III was not included (middle model in Fig. 7) is not unique in the synthetic spectrum and therefore the identification of C III can not be considered definitive.

A possible alternative to C III would be H. In order to achieve a good agreement with the data at 4500 Å the optical depths and velocity range needed would produce a strong Hα line in the Si II $\lambda 6355$ (as shown in Fig. 8) region because of the resonance scattering approximation with used by SYNOW to compute the sourse function of this line. . The SYNOW parameters used for H are: v_{min}=25$\times 10^3$ km s^{-1}, v_{max}=40$\times 10^3$ km s^{-1}, τ=0.8, T_{exc}=15$\times 10^3$ K and v_e=5$\times 10^3$ km s^{-1}. Note however, that as discussed in Thomas et al. (2003) considering the net emission effect the strength of the Hα line could be weaken. Yet another possibility would be He II. This would indeed produce a good agreement with the observed feature. However, the high degree of non-thermal ionization needed to produce this absorption makes this option appear less plausible, unless a big amount of radioactive material could be proved to be present in the external layers of SN 1999ac. Ni III is used in the synthetic spectrum to improve the matching in the 4700 Å and 5300 Å region. Because of the absence of Co III lines we consider this ion coming from stable ^{58}Ni.

Day -9

Fig. 9 shows the synthetic spectrum produced for matching the data at day 9 before maximum light using the parameters shown in table 3. The ions used here are the same as for the previous epoch. The line profile of Si II λ6355 is no longer reproduced by a detached layer.

At this epoch C II is needed in order to match the red edge of the Si II line at 6150 Å and it is introduced with the same velocity range as in day −15. The two lines have now blended together because of the lower minimum velocity of Si II. Fig. 10 shows the 6150 Å region and the contribution of the C II to the match of the synthetic spectrum. Due to the small optical depth of C II its contribution at 4500 Å and 7000 Å appears very weak in the synthetic spectrum.

A small absorption on the P-Cygni emission of Si III λ4500 can be matched also at this epoch with the introduction of C III at photosphere velocities. Fig. 11 shows the highlight of the 4500 Å region and the C III contribution. The identification of C III is as controversial as for day −15 although no better alternatives were found. A firm identification may be possible only through NLTE calculations.

Read only quickly b/c suspicious of "C II" ~ λ7000Å since telluric lines not corrected

5.   Expansion Velocities

The Doppler shift of the minimum of a line is a measurement of the velocity at which the ion responsible for the line produces the maximum absorption and can be used to investigate the inner structure of the expanding atmosphere and its time evolution.

Fig. 12 and 13 show the velocities inferred from the minima of Ca II H&K and Si II λ6355. The measurements have been obtained performing a non-linear fit with a Gaussian model to the whole line profile. When a line showed some contamination from

other ions and thus was not well represented by a Gaussian profile the fit was limited to a smaller region in the vicinity of the minimum. The statistical errors of the fit are within few km s^{-1} and thus too small to be plotted on the graphs.

The velocity of Ca H&K is not available before maximum light since the spectra do not cover completely this feature. From day 0 and beyond, the values decrease monotonically following the evolution of the other SNe Ia. Overall, SN 1999ac shows relatively high Ca H&K velocities.

The time evolution of the velocity of Si II, shown in Fig. 13, is instead more peculiar. The general trend for normal type Ia supernovae is to show rapidly decreasing Si II velocities during the first two weeks after the explosion (approximately up to one week before maximum light) and slower decline rate after maximum light. SN 1999aa-like supernovae show Si II blue shift approximately constant in time at least up to 40 days past maximum (Garavini et al. 2003). Under-luminous objects (e.g: SN 1999by or SN 1991bg) show instead constantly decreasing velocities.

contamination?

SN 1999ac has many spectral characteristics similar to SN 1999aa-like objects but the Si II velocities are similar or inferior to objects such as SN 1999by and SN 1991bg. This trend is unique among the SNe with similar spectro-photometric characteristics.

6. Conclusions

We have presented spectroscopy observation of SN 1999ac between −15 and 42 days from B-band maximum. The overall evolution shows peculiarities resembling a SN 1999aa-like object with a faster transition toward a normal looking spectrum. In the early spectra Si II $\lambda6355$ and Ca II H&K – characteristic of Branch-normal supernovae – are visible and strong while Fe III $\lambda\lambda4404,5129$ – characteristic of genuine SN 1991T-like objects – are

present but weak.

We performed direct spectroscopic analysis of pre-maximum (day −15 and day −9) spectra of SN 1999ac. The inferred composition is schematically drawn in Fig. 14

The spectrum at day −15 shows an absorption feature on the red side of Si II $\lambda6355$ that can be reproduced by the SYNOW synthetic spectra introducing a detached layer of C II $\lambda6580$. The identification of C II is also supported by the absorption feature around 7000 Å and the small contribution at 4500 Å. At day −9, as the photosphere recedes further into the atmosphere, C II $\lambda6580$ blends with Si II $\lambda6355$ and its contribution becomes less evident. The velocity range at which C II appears ($v>16000$ km s^{-1}) is consistent with predictions from a pure deflagration explosion.

The small absorption on the red edge of Si III $\lambda4560$ may be reproduced in the synthetic spectrum as C III $\lambda4648.8$ extending down to photosphere velocity. The possible contribution of C III is still visible at day −9. This identification is not definitive since C III does not form distinctive lines. We also attempt to reproduce this absorption with Hβ. This would produce a mismatch in the Si II $\lambda6355$ region due to Hα. Note however, that our calculation is based on a pure resonance scattering source function and therefore the Hα line can result over-strengthen. If NLTE calculations would confirm the identification of C III it would imply that the original C+O composition can be found at the same radii as the intermediate mass elements in SN1999ac. Thus, 3D modeling would probably be necessary to reproduce the observations.

The analysis of the time evolution of velocities as derived from the minima of Ca II H&K SN 1999ac shows a trend consistent with normal type Ia's with values slightly higher than average. The velocities deduced from Si II $\lambda6355$ show monotonically decreasing values that follow the trend of under-luminous supernovae. This characteristic is unique for this object, otherwise showing many similarities to the slow decliner SN 1999aa.

The range of diversities in the spectral and photometric characteristics of SNe Ia is
constantly broadening. SN 1999ac ~~represents~~ *is* yet another ~~example~~ *demonstration* that all supernovae can
not be described only by a ^{56}Ni-temperature sequence, but that a complete model has to
take into account also asymmetries, interaction with the companion star and probably
complex 3D hydrodynamics. *None of this was shown here*

---

[30]http://www.nhn.ou.edu/~suspect

REFERENCES

Aldering, G. 2000, "Type Ia Supernovae & Cosmic Acceleration," *AIP Conference Proceeding: Cosmic Explosions*, ed. S. S. Holt & W. W. Zhang, Woodbury, New York: American Institute of Physics

Arbour, R. 1999, IAU Circ. 7108

Arnett, W. D., 1969 ApJS, 5, 180.

Baron, E., Lentz, Eric J., Hauschildt, Peter H., 2003, ApJ, 588L, 29B

Branch, D., Lacy, C. H., McCall, M. L., et al. 1983, ApJ, 270, 123B

Branch, D., Fisher, A., Nugent, P., 1993, AJ 106, 2383

Branch, D. 2000, astro-ph/0012300

Branch, D., Baron, E., Jeffery, J. D. 2001, astro-ph/0111573

Branch, D. 2001 PASP,113,169B

Branch, D., Garnavich, P., Matheson, T. 2003, astro-ph/0305321

Cardelli, J. A., Clayton, G. C., Mathis, J. S. 1989, ApJ, 345, 245

Castor, J. I. 1970, MNRAS, 149, 111

Filippenko A. V. Richmond, M. W.; Matheson, T., et al. 1992 ApJ, 384, L15

Filippenko, A. V. 1997 ARA&A, 35, 309F

Filippenko, A. V., Li, W. D., Leonard, D. C. 1999, IAU Circ. 7108

Fisher, A., Branch, D., Hatano, K., Baron, E. 1999, MNRAS, 304, 67

Fisher, A., Branch, D., Nugent, P., Baron, E., et al. 1997, ApJ, 304, L89

Folatelli et al. 2003, in prep.

Gamezo, V. N., Khokhlov, A. M., Oran, E. S., Chtchelkanova, A. Y., Rosenberg, R. O. 2003 Sci, 299, 77G

Garnavich, P. M., Bonanos A. Z., Jha S., et al. 2001, astro-ph/0105490

Gibson, B. K., Stetson, P. B. 2001, ApJ, 547L, 103G

Gomez, G., Lopez, R., Sanchez, F. 1996 AJ, 112, 2094G

Hamuy, M., Phillips, M. M., Maza, J., et al. 1995, AJ,109,1H

Hamuy, M., Phillips, M. M., Suntzeff, N. B., et al. 1996, AJ, 112, 2391H

Hamuy, M., Trager, S. C., Pinto, P. A., et al. 2000, AJ, 120, 1479H

Mario Hamuy, M. M. Phillips, Nicholas B. Suntzeff, et al.,2003, astro-ph/0306270

Hansen, Carl J.; Wheeler, J. Craig, 1969, Ap&SS, 3, 464H

Hatano, K., Branch, D., Fisher, A., Millard, J., Baron, E., 1999, ApJ, 121, 233

Hatano, K., Branch, D., Fisher, A., Baron, E., Filippenko, A. V., 1999, ApJ, 525, 881

Hatano, K., Branch, D., Qiu, Y. L., et al. 2002, NewA,7,441H

Hatano, K., Branch, D., Qiu, Y.L., Baron, E., Thielemann, F.-K. 2002, NewA, 7, 441

Hillebrandt, W., Niemeyer, J. C. 2000, ARAA, 38, 191

Hoyle F., Fowler, W. A., 1960 AJ, 132, 565

Horne, K. 1986, PASP, 98, 609

Howell, D. A. 2001, ApJ, 554L, 193H

Howell, D. A., Höflich, P. Wang, L., Wheeler, J. C. 2001, ApJ, 556, 302H

Howell, D. A. in preparation.

Höflich, P., Wheeler, J. C., Thielamann, F.-K. 1998, ApJ, 495, 617

Iben, I. Jr., Tutukov, A. V. 1984, ApJS, 54, 335I

Iwamoto K., Brachwitz F., Nomoto K., et al., 1999, ApJS, 125

Jeffrey, D. J.,Branch, D., 1990, Supernovae, Jerusalem Winter School for Theoretical
        Physics

Jeffrey, D. J., Leibundgut, B., Kirshner, R. P., et al. 1992, ApJ, 397, 304

Jha, S., Garnavich, P. M., Kirshner, R. P., et al. 1999, ApJS, 125, 73J

Jha, S., 2002 PhD thesis , Harvard University

Kasen, D., Nugent, P., Wang, L., et al. 2003, ApJ, 593, 788

Khokhlov, A.M., 1991, A&A, 245, 114

Khokhlov, A.M., 2000, astro-ph/0008463

Kirshner R. P. Jeffery, D. J., Leibundgut, B., et al. 1993 ApJ, 415, 589

Kiss, L., Sarneczky, K., Yoshida, S., Kadota, K., 1999, IAUC, 7122, 3K

Krisciunas, K., Hastings, N.G., Loomis, K., et al. 2000 ApJ, 539, 658

Kurucz, R., 1993, Atomic data for opacity calculations. Kurucz CD-ROM No. 1. Cambridge,
        Mass.: Smithsonian Astrophysical Observatory.

Leibundgut, B. 2000, A&AR, 10, 179

Leibundgut, B., Kirshner, R. P., Filippenko, A. V., et al. 1991, ApJ, 371 L23

Lentz, E.J., Baron, E., Branch, D., Hauschildt, P.H., Nugent, P., 2000, ApJ, 530, 966-976.

Lentz, E. J.; Baron, E. Hauschildt, P. H., Branch, D., 2002, ApJ, 580, 374L

Lentz E.J., Baron E., Branch D., Hauschildt P.H., 2001, ApJ, 547, 402.

Li, W.D., Qiu, Y. L., Qiao, Q. Y., et al. 1999 ApJ 117, 2709

Li, W.D., Filippenko, A. V., Gates, E., et al. 2001a, PASP, 113, 1178

Li, W.D., Filippenko, A. V., Treffers, R. R., et al. 2001b, ApJ, 546, 734

Li, W., 2002, IAUC, 7898, 2L

Li, W., Filippenko, A. V., Chornock, R., e. al., 2003, PASP, 115, 453L

Mario Livio,2000,astro-ph/0005344

Livio, M., Riess, A., 2003, astro-ph/0308018

Livne, Eli,1990, ApJ, 354L, 53L

Livne, Eli, Glasner, Ami S., 1991, ApJ, 370, 272L

Marietta, E., Burrows, A., Fryxell, B., 2000, ApJS, 128, 615M

Marquardt Donald W.,J. Soc. Indust. Appl. Math. Vol. 11. No. 2, June 1963

Mazzali, P. A., Lucy, L. B., Danziger, I. J., et al., 1993, A&A, 269, 423

Mazzali, P.A, Danzinger, I.J., Turatto, M. 1995 A&A, 297, 509

Mazzali, P. A., Cappellaro, E., Danziger, I. J., Turatto, M., Benetti, S., 1998, ApJ, 499L, 49M

Mazzali, P. A. 2001 MNRAS, 321, 341

Modjaz, M., King, J. Y., Papenkova, M. et al., 1999 IAUC, 7114,1M

Nakano, S., & Kushida, R. 1999, IAU Circ. 7109

Nomoto, K.; Sugimoto, D.; Neo, S., 1976, Ap&SS, 39L, 37N

Nomoto, K. 1982, ApJ, 257, 780N

Nomoto, K., Thielemann, F.-K., Yokoi, K. 1984, ApJ, 286, 644

Nugent, P., Phillips, M., Baron, E., Branch, D., Hauschildt, P.H. 1995, ApJ, 455, 147

Nugent, P., Baron, E., Branch, D., Fisher, A., Hauschildt, P.H. 1997, ApJ, 485, 812

Nugent, P., Aldering, G., & The Nearby Campaign 2000, Supernovae and gamma-ray bursts: The Greatest Explosions Since the Big Bang: poster papers from the Space Telescope Science Institute Symposium, May 1999 / Mario Livio, Nino Panagia, Kailash Sahu, editors. [Baltimore, Md.] : Space Telescope Science Institute, [2000]., p.47, 47.

Patat, F., Benetti, S., Cappellaro, E., et al. 1996, MNRAS, 278, 111-124.

Paczynski, B., 1985, cvlm.proc, 1P

Phillips, M. M., Wells, L. A., Suntzeff, N. B., et al. 1992, AJ,103, 1632P

Phillips, M. M., Lira, P., Suntzeff, N. B., et al. 1999, AJ, 118, 1766

Phillips, M. M., Kunkel, W., Filippenko, A. V., 1999, IAUC, 7122, 2P

Phillips M. M.,Krisciunas K.,Suntzeff N. B., et al., astro-ph/0211100

Qiao, Q. Y., Wei, J. Y., Qiu, Y. L., Hu, J. Y., 1999, IAU Circ. 7109

Ruiz-Lapuente, P., Cappellaro, E., Turatto, M., et al. 1992, ApJ, 387L, 33R

Saha, A., Sandage, A., Thim, F., et al. 2001, ApJ, 551, 973S

Salvo, M. E., Cappellaro, E., Mazzali, P. A., et al. 2001, MNRAS, 321, 254S

Schlegel, D. J., Finkbeiner, D. P., Davis, M. 1998, ApJ, 500, 525

Sobolev, V. V. 1960, Moving Envelopes of Stars (Cambridge: Harvard Univ. Press)

Strolger, L.-G., Smith, R. C., Suntzeff, N. B. et al., 2002, AJ, 124, 2905S

Theureau, G., Bottinelli, L., Coudreau-Durand, N., et al. 1998, A&AS, 130, 333T

Thomas, R. C., Branch, D., Baron, E., et al., 2003, astro-ph/0302260

Thomas, R. C., Kasen, D. Branch, D., B., E., 2002, ApJ, 567, 1037T

Wang L., Baade D., Hoeflich, P., Khokhlov, A., Wheeler, J.G. et al., 2003, ApJ, 591, 1110,
    1128

Wells, L. A., Phillips, M. M., Suntzeff, B., et al. 1994, AJ, 108, 2233W

Whelan, J., & Iben, I. Jr. 1973, ApJ, 186, 1007W

Woosley; S. E., Weaver; T. A. 1986 ARA&A 24, 205.

Woosley, S. E., Weaver, T. A., 1994, ApJ, 423, 371W

Yamaoka; H., Nomoto; K., Shigeyama; T., Thielamann; F.-K. 1992, ApJ, 393,55.
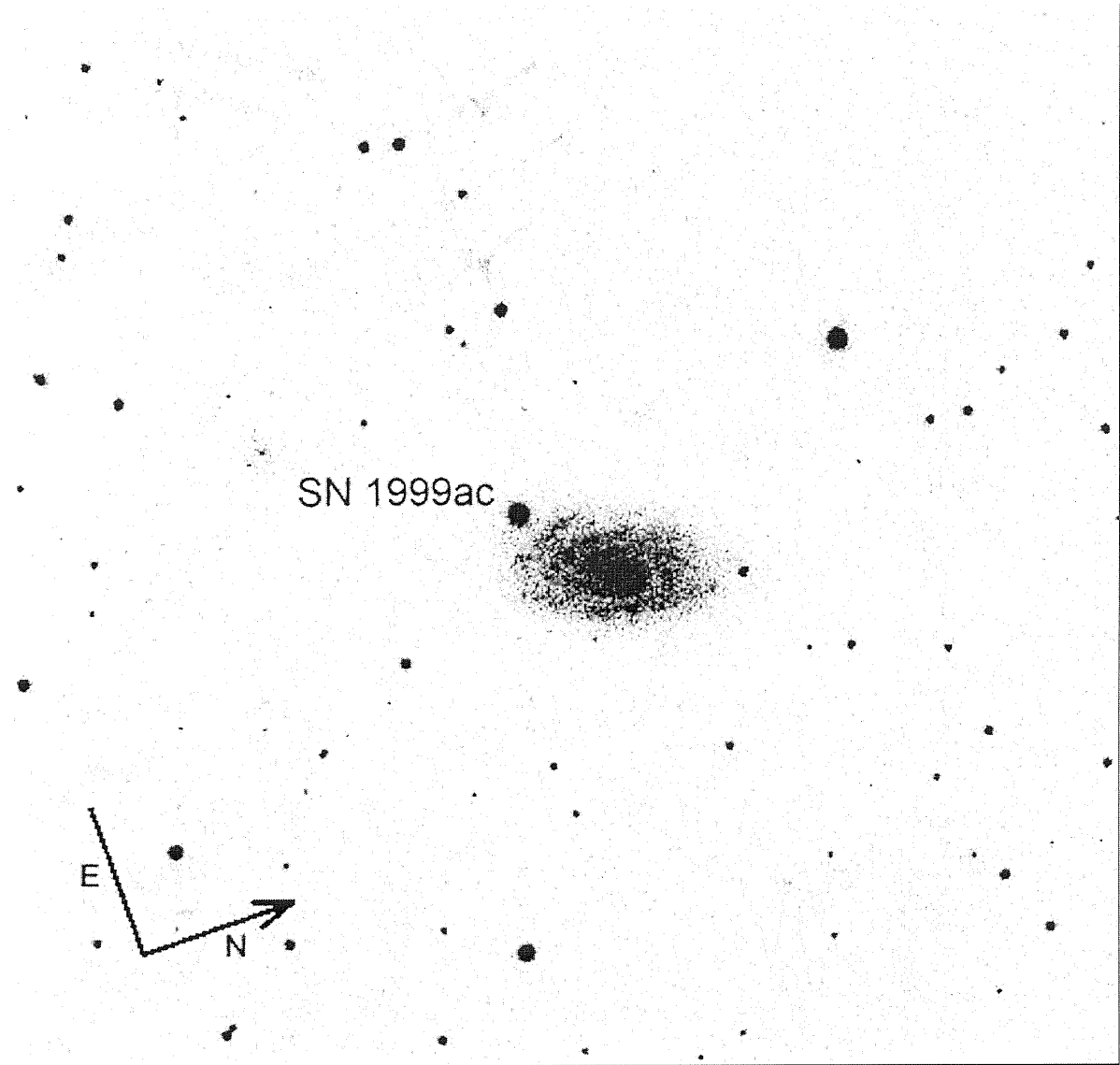
Fig. 1.— SN 1999ac in its host galaxy R.A. = $16^h07^m15.0^s$ Decl. = $+07^d58^m20^s$ (equinox 2000.0). B-band image obtained at NOT on 1999 March 15 UT with SN 1999ac indicated. The field is $6'.5$ across.
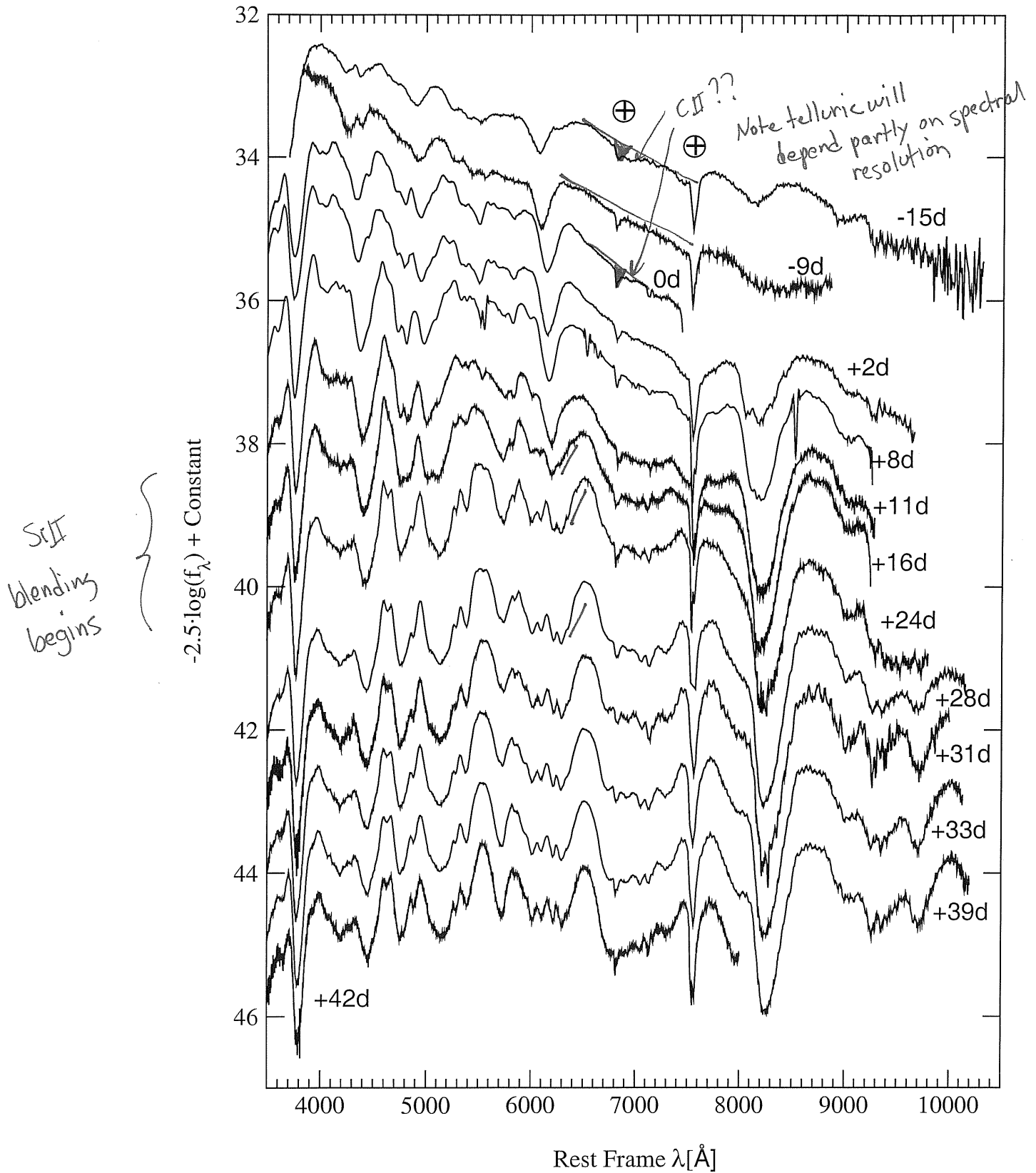
Fig. 2.— SN 1999ac spectral time evolution. Epochs referred to B-band maximum light. The ⊕ symbol marks the atmospheric absorptions.
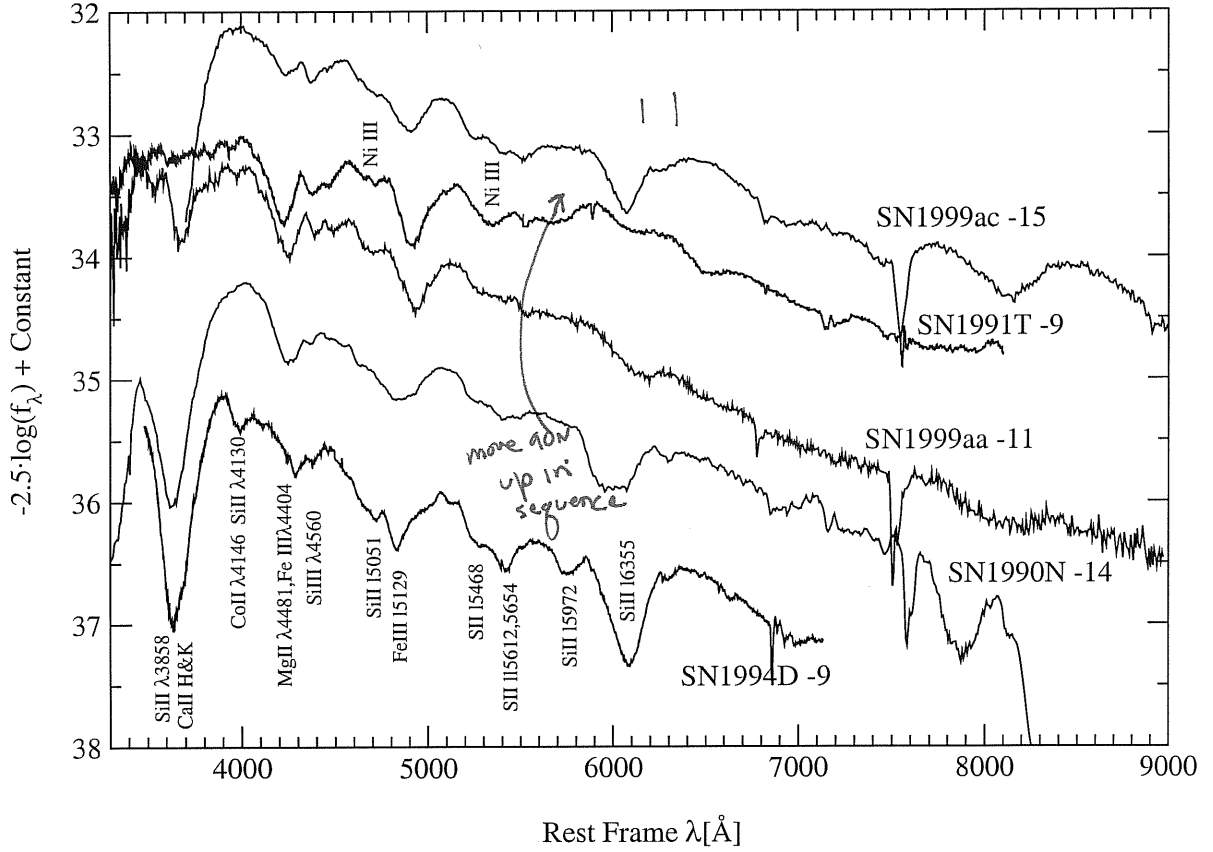
Fig. 3.— The −15 days spectrum of SN 1999ac together with those of SN 1999aa, SN 1991T, SN 1990N and SN 1994D respectively from Garavini et al. (2003); Filippenko (1992); Leibundgut et al. (1991); Patat et al. (1996). Epochs are quoted in the labels. Line identification are taken as in Li et al. (1999, 2001a); Fisher et al. (1999); Patat et al. (1996); Mazzali et al. (1995); Kirshner et al. (1993); Jeffrey et al. (1992).
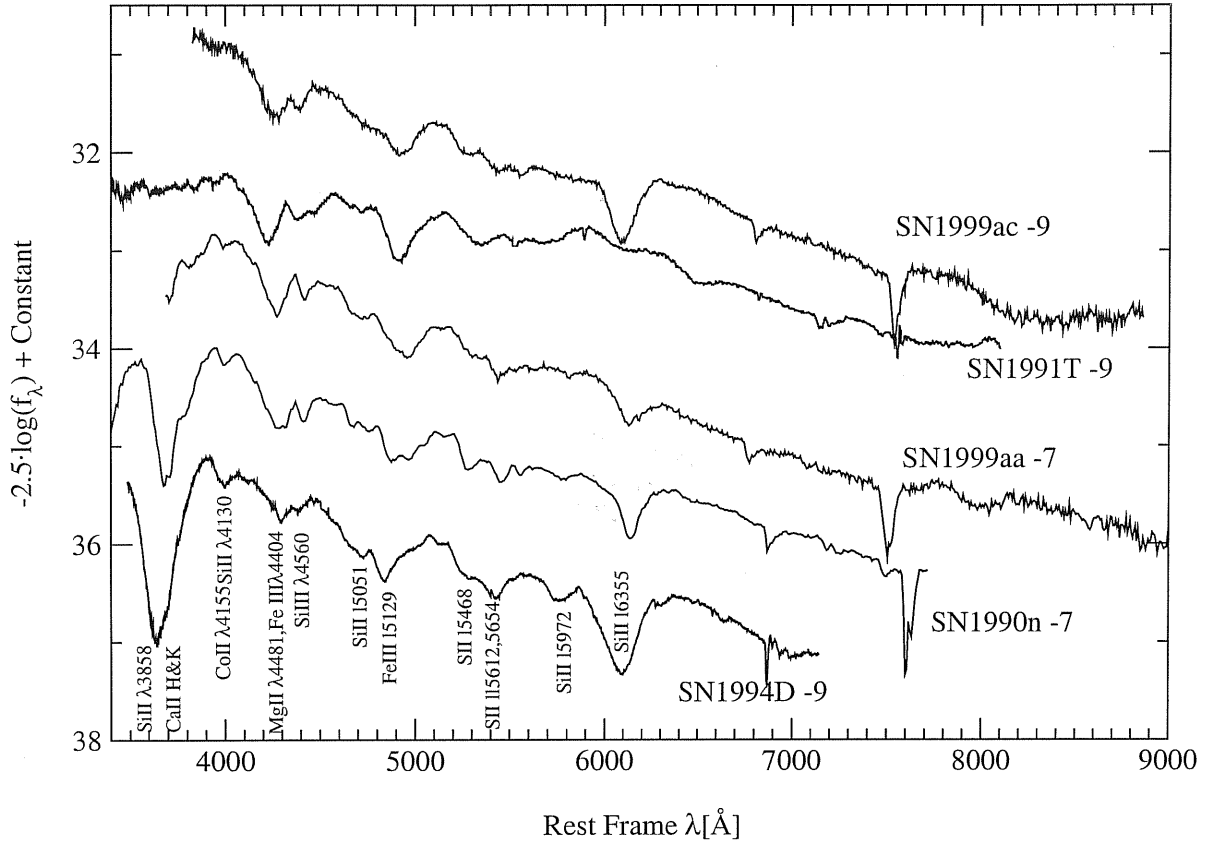
Fig. 4.— The −9 days spectrum of SN 1999ac together those of SN 1999aa, SN 1991T, SN 1990N and SN 1994D Garavini et al. (2003); Filippenko (1992); Leibundgut et al. (1991); Patat et al. (1996). Epochs are quoted in the labels. Line identification are taken as in Li et al. (1999, 2001a); Fisher et al. (1999); Patat et al. (1996); Mazzali et al. (1995); Kirshner et al. (1993); Jeffrey et al. (1992).
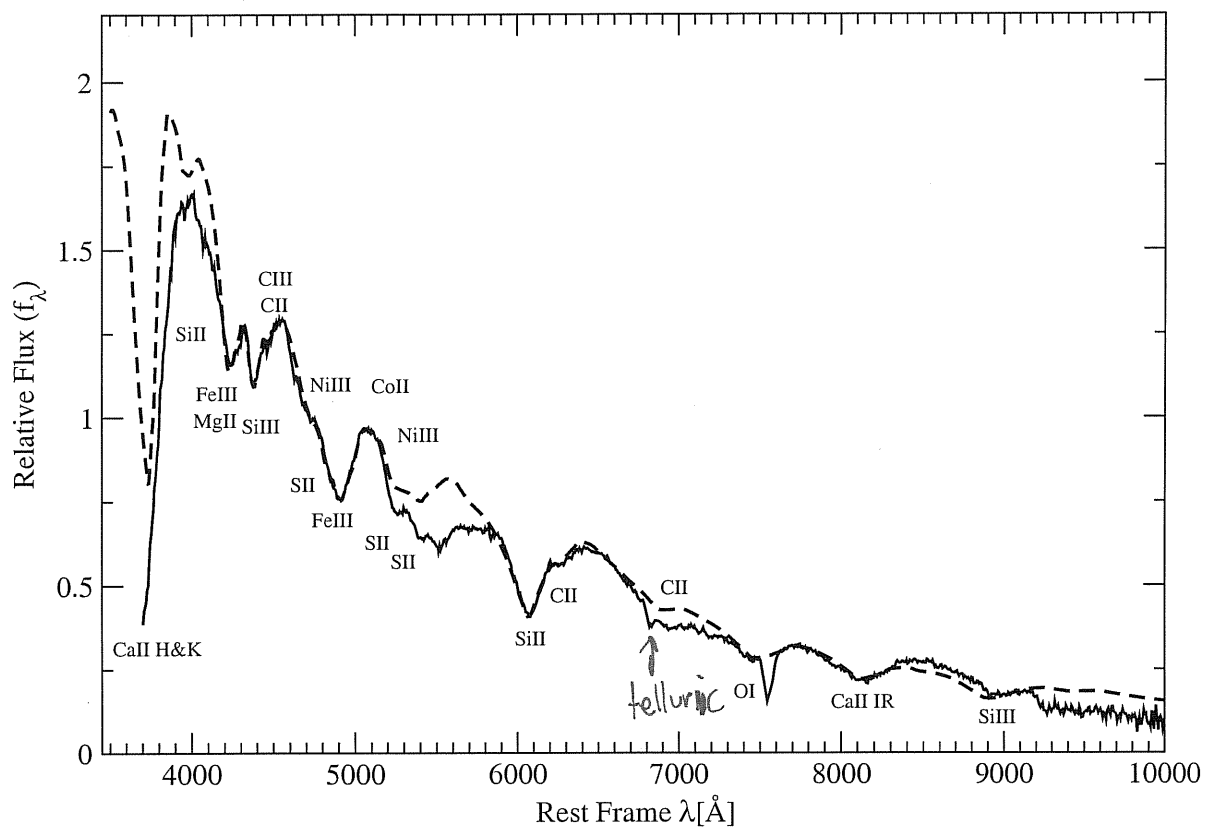
Fig. 5.— Synthetic spectra compared with SN 1999ac spectrum for −15 days. Dashed line: best match synthetic spectrum. Solid line: data. SYNOW parameters used are presented in table 2. Ions responsible for features in the synthetic spectrum are marked.
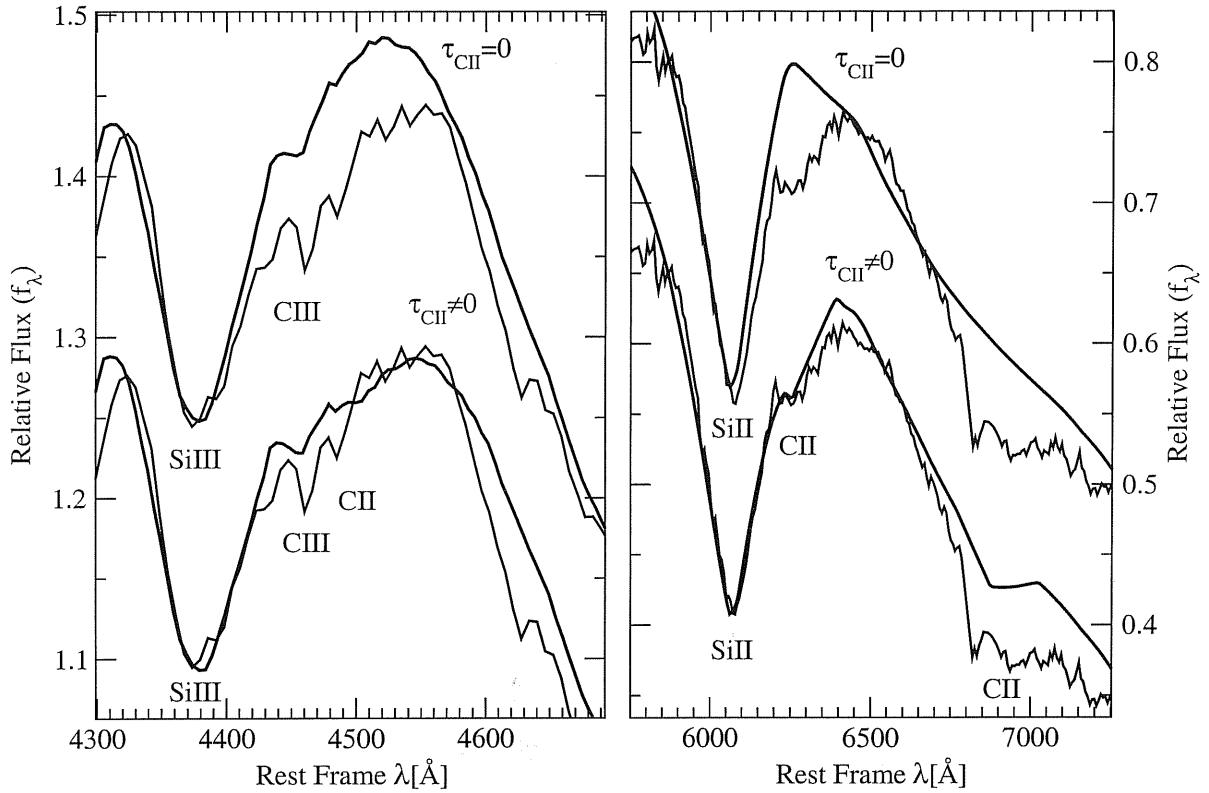
Fig. 6.— Synthetic spectra compared with SN 1999ac spectrum for -15 days in the 4500 Å (left panel) and 6150 Å (right panel) region. First model from the top: Solid lines $\tau_{CII} = 0$ and data; Second model from the top: Solid lines $\tau_{CII} \neq 0$ and data. SYNOW parameters used are presented in table 2. Ions responsible for features in the synthetic spectrum are marked.

Must do telluric correction to demonstrate any feature at 6900Å.

I thought we have been though this same issue many times before. Why hasn't it been resolved?
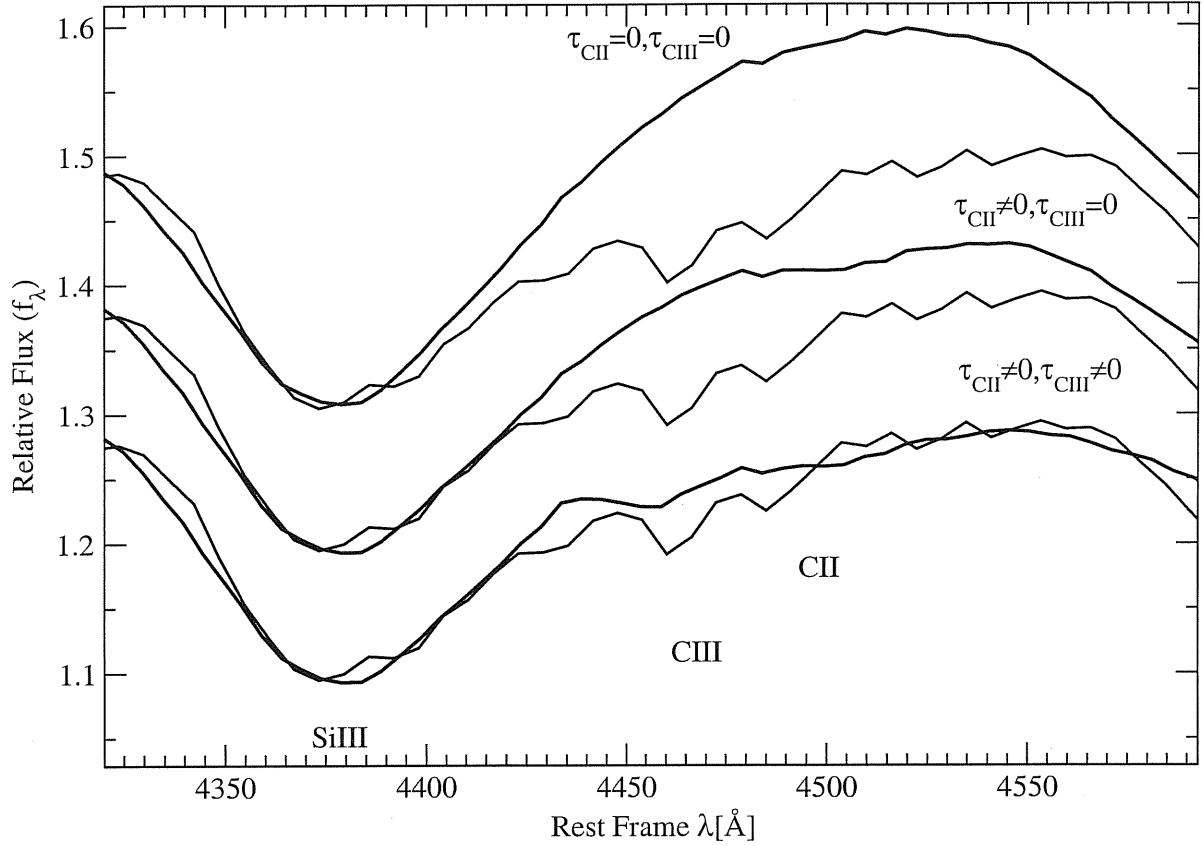
Fig. 7.— Synthetic spectra compared with SN 1999ac spectrum for −15 days in the 4500 Å region. First model from the top: Solid lines $\tau_{CIII} = 0$, $\tau_{CII} = 0$ and data; Second model from the top: Solid lines $\tau_{CIII} = 0$, $\tau_{CII} \neq 0$ and data; Third model from the top: Solid lines $\tau_{CIII} \neq 0$, $\tau_{CII} \neq 0$ and data. SYNOW parameters used are presented in table 2. Ions responsible for features in the synthetic spectrum are marked.
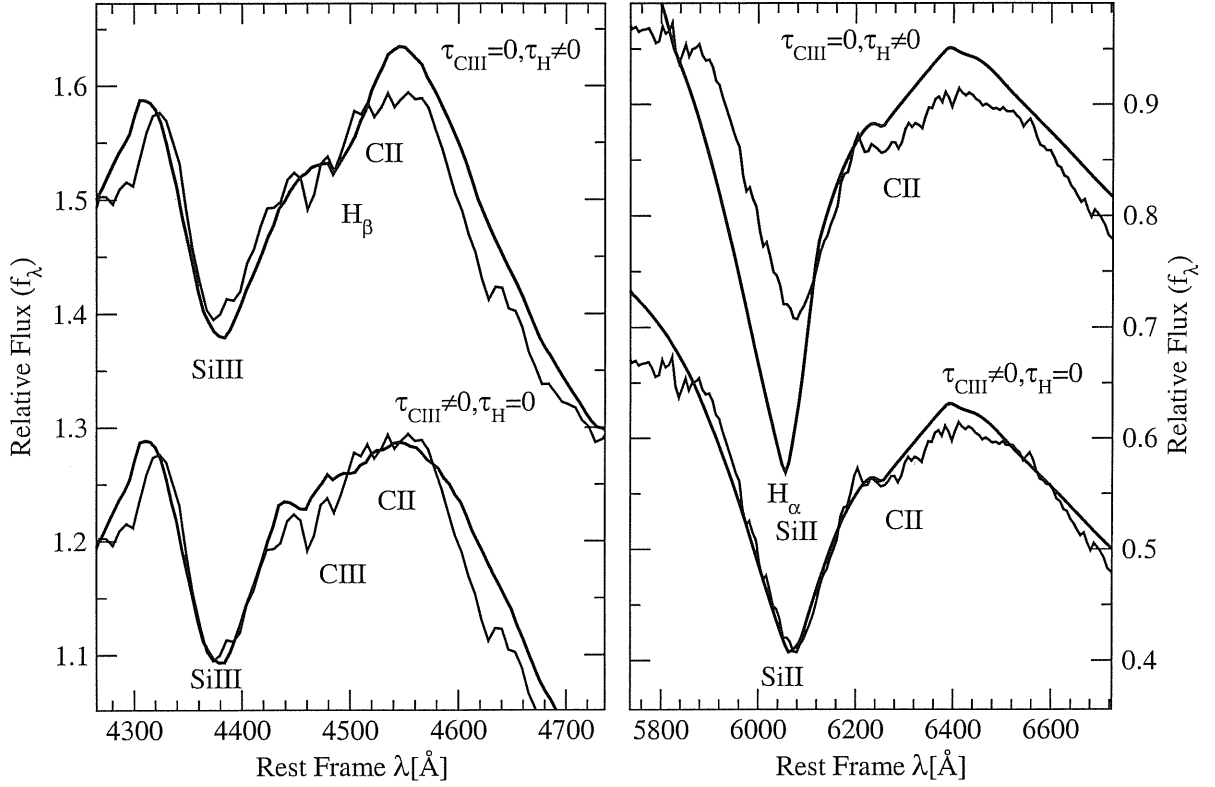
Fig. 8.— Synthetic spectra compared with SN 1999ac spectrum for −15 days in the 4500 Å (left panel) and 6150 Å (right panel) region. First model from the top: Solid lines $\tau_{\text{CIII}} = 0, \tau_H \neq 0$ and data; Second model from the top: Solid lines $\tau_{\text{CIII}} \neq 0, \tau_H = 0$ and data. SYNOW parameters used are presented in table 2 and in the text. Ions responsible for features in the synthetic spectrum are marked.
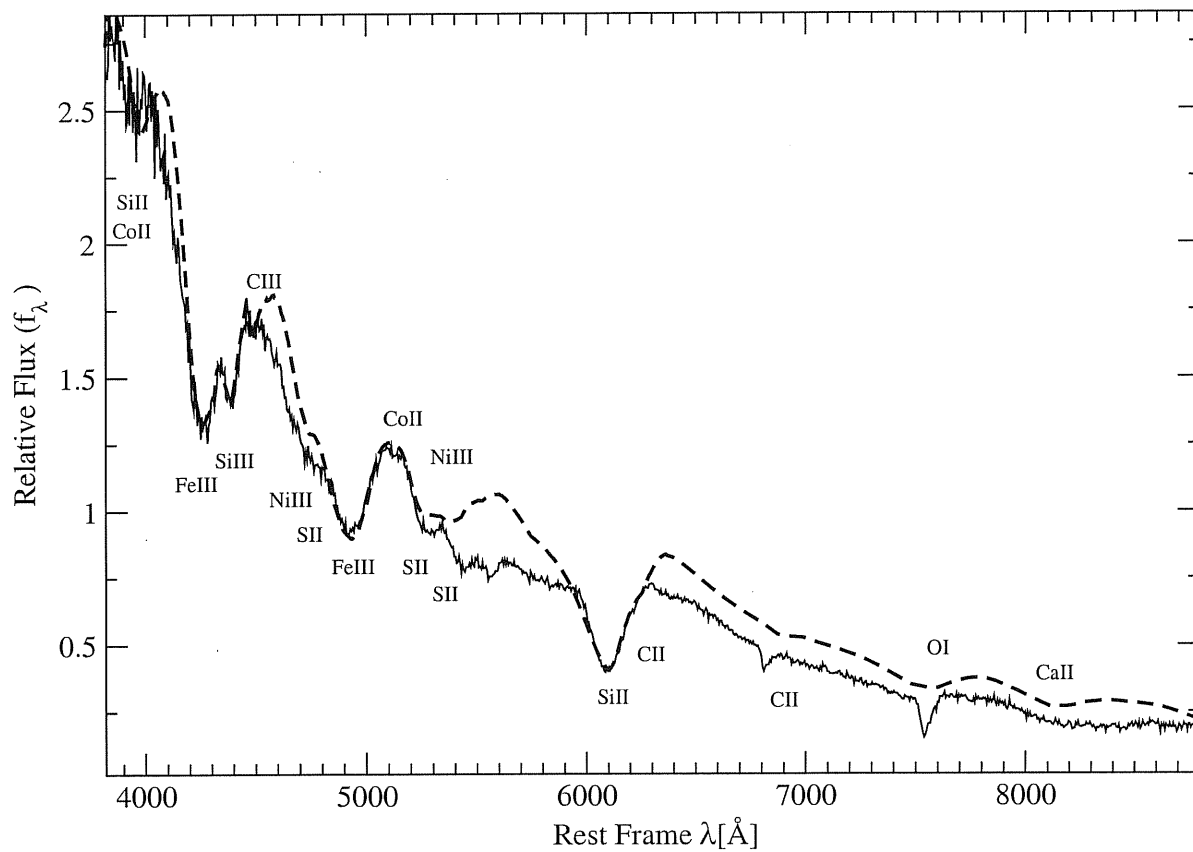
Fig. 9.— Synthetic spectra compared with SN 1999ac spectrum for −9.days Dashed line: best match synthetic spectrum. Solid line: data. SYNOW parameters used are presented in table 3. Ions responsible for features in the synthetic spectrum are marked.
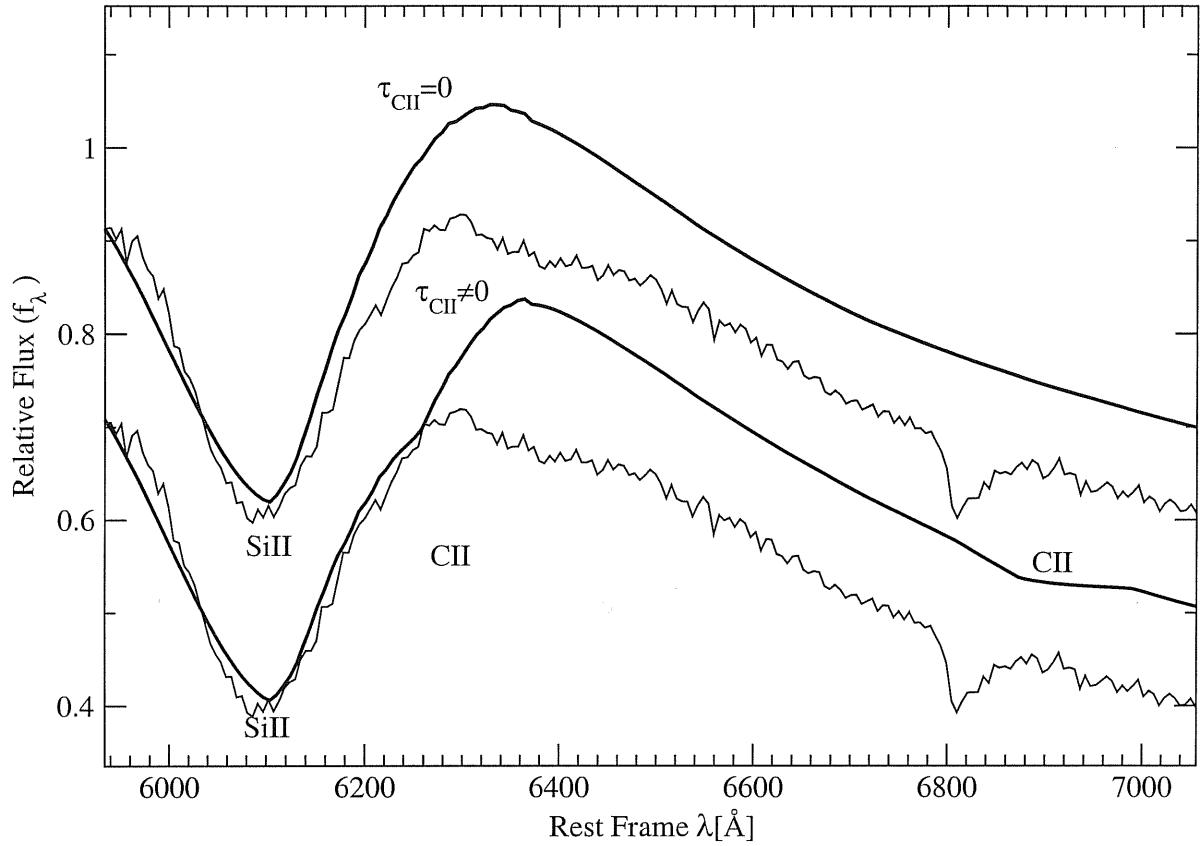
Fig. 10.— Synthetic spectra compared with SN 1999ac spectrum for −9 days in the 6150 Å region. First model from the top: Solid lines $\tau_{CII} = 0$ and data; Second model from the top: Solid lines $\tau_{CII} \neq 0$ and data. SYNOW parameters used are presented in table 3. Ions responsible for features in the synthetic spectrum are marked.
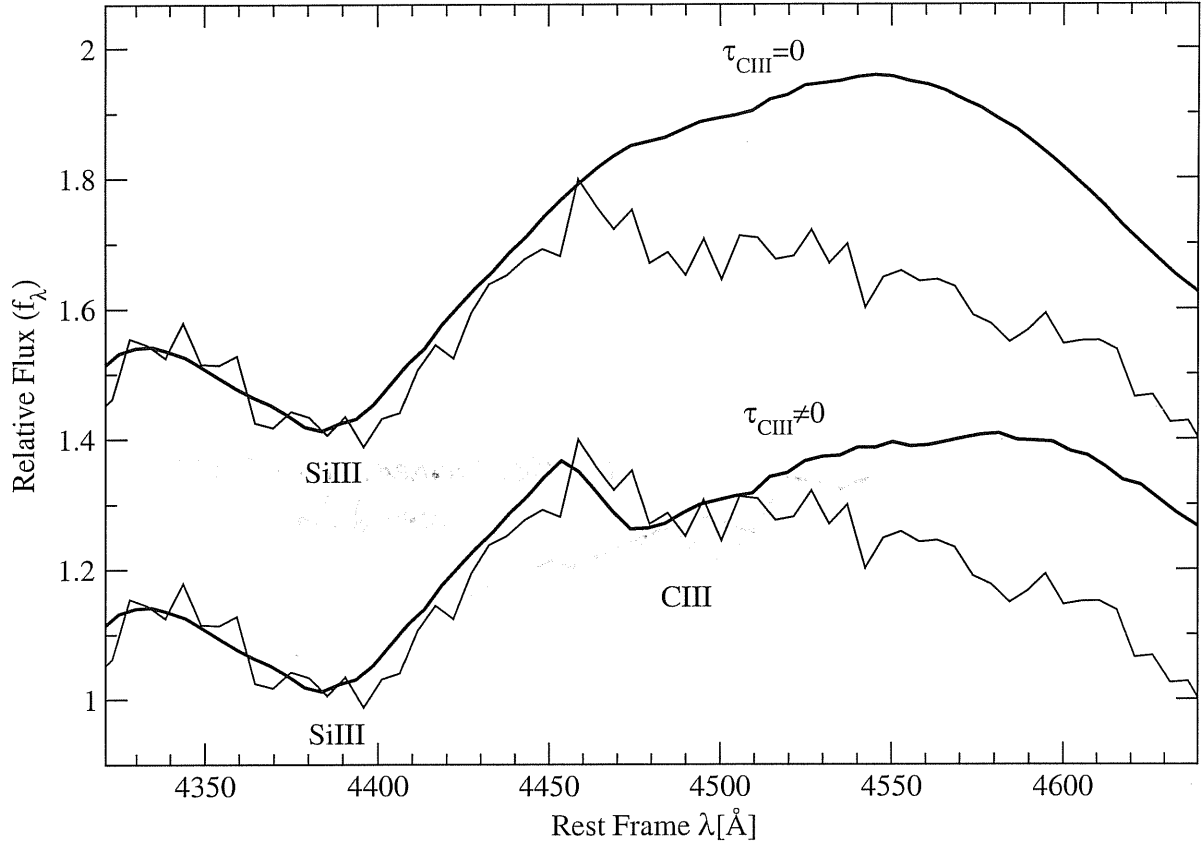
Fig. 11.— Synthetic spectra compared with SN 1999ac spectrum for −9 days in the 4500 Å region. First model from the top: Solid lines $\tau_{CIII} = 0$ and data; Second model from the top: Solid line $\tau_{CIII} \neq 0$ and data. SYNOW parameters used are presented in table 3. Ions responsible for features in the synthetic spectrum are marked.
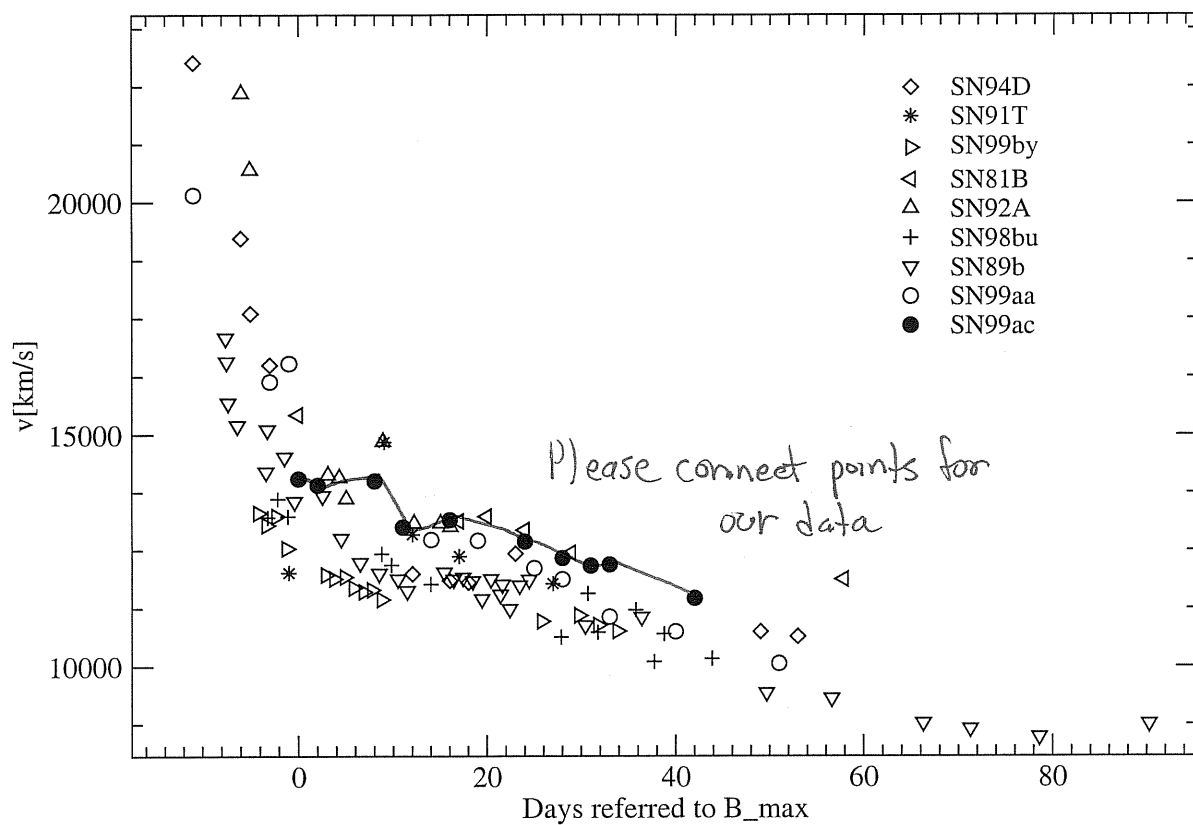
Fig. 12.— Expansion velocities of SN 1999ac as inferred from the minima of Ca II H&K compared with the values of other SNe taken from Wells et al. (1994); Garnavich et al. (2001); Kirshner et al. (1993); Patat et al. (1996); Jha et al. (1999) and references therein. Values for SN 1999ac are marked as filled circles.
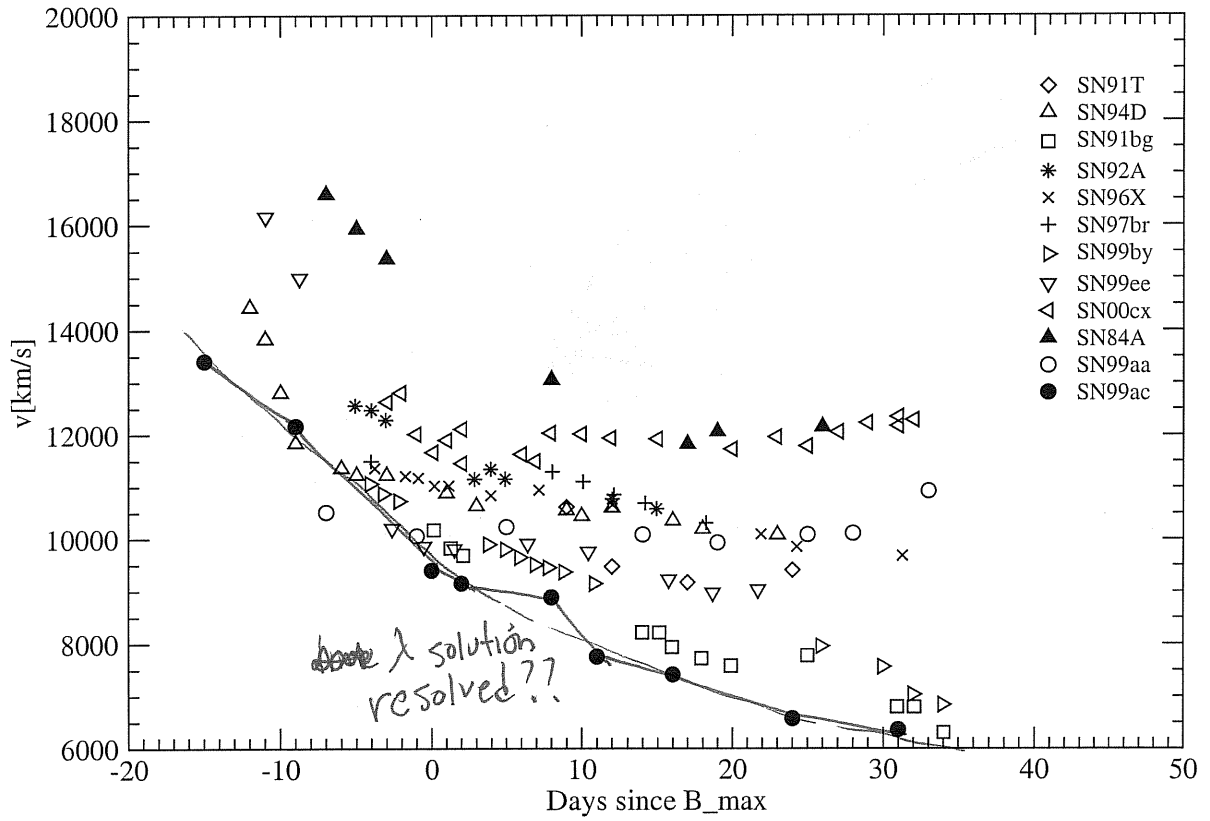
Fig. 13.— Expansion velocities of SN 1999ac as inferred from the minima of Si II $\lambda6355$ compared with the values of other SNe taken from Li et al. (1999, 2001a); Garnavich et al. (2001); Salvo et al. (2001) and references therein. Values for SN 1999ac are marked as filled circles.
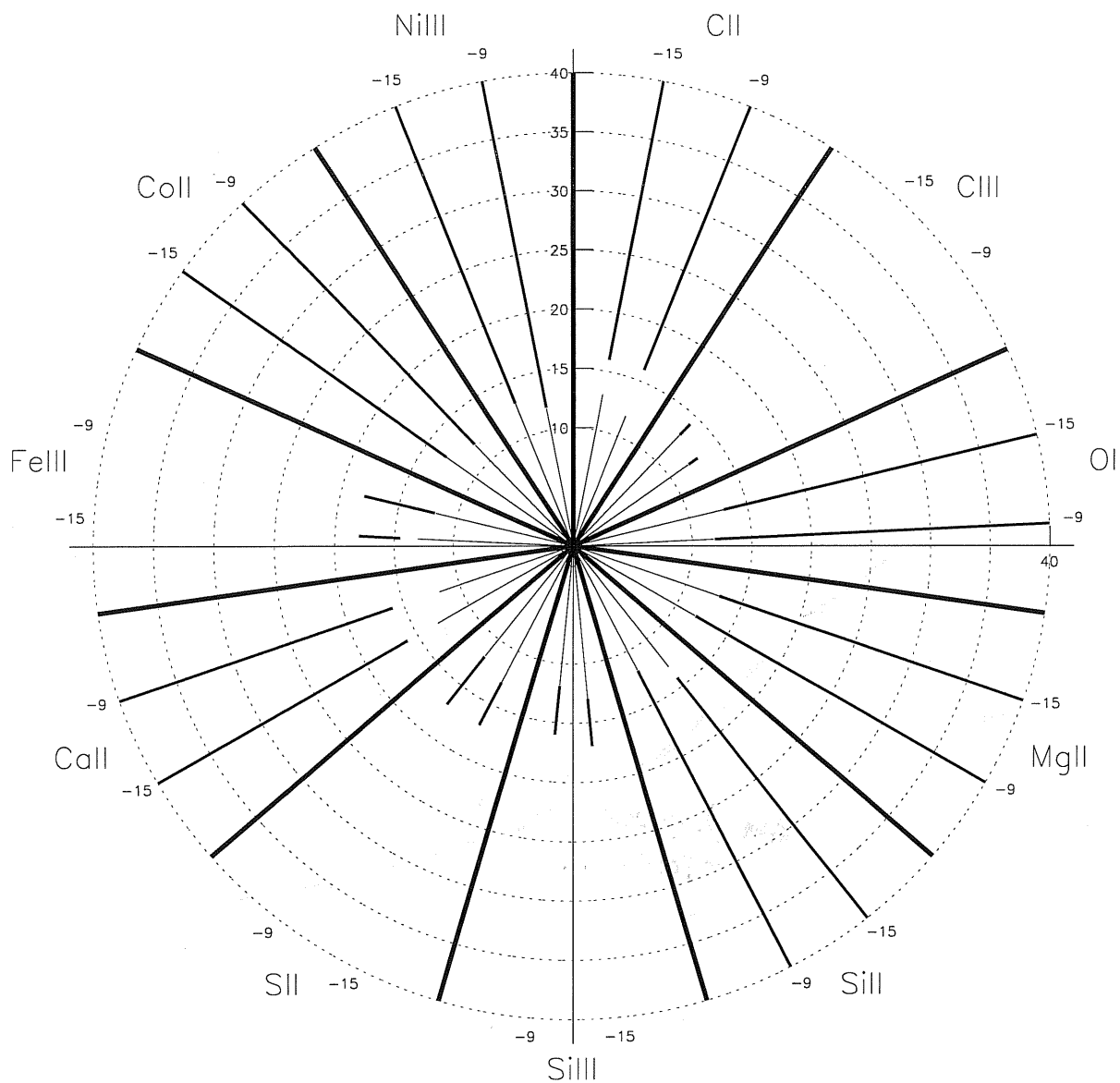
Fig. 14.— Schematic representation of the composition of SN 1999ac in velocity space as inferred from the SYNOW synthetic spectra of -15, -9 days. Velocities increase radially in units of 10^3 km s^{-1}. The velocity ranges (v_{min}-v_{max}) for 11 ion species used in the synthetic spectra are marked with solid lines inside the circle section labeled with the ion name. High velocities components are marked with dashed lines. In each ion section the 2 epochs analysed are shown. For each epoch the photosphere extension is market with a thin solid line. For details see section 4.

Table 1: Data set specifications.

Handwritten annotation: "Should quote resolution (use arc or unblended sky lines"

JD −2400000	Epoch[f] [ref B_{max}]	Telescope	Instrument	λ Range[f] [Å]	$\langle\Delta\lambda\rangle^a$ [Å]	$\langle S/N\rangle^b$	Comments
51236.89	−15	APO	DIS	3703-10307	6.8	125	5696.16 [c]
51240.95	−9	MDM 2.4m	MARK III	3827-8860	5.4	63	[e]
51251.39	+0	ESO 3.5m	EFOSC	3331-7495	4.0	325	[d]
51253.84	+2	CTIO 4m	RCSP	3235-9263	2.0	76	[d]
51253.72	+2	NOT	ALFOSC	3285-9655	6.2	176	5852.06[c]
51259.88	+8	CTIO 4m	RCSP	3227-9254	2.0	94	[d]
51262.89	+11	CTIO 4m	RCSP	3254-9278	2.0	114	[d]
51267.87	+16	CTIO 4m	RCSP	3239-9241	2.0	90	[d]
51275.98	+24	KPNO 4m	T2KB	3029-10401	5.4	59	[d]
51279.85	+28	ESO 3.6m	EFOSC	3341-10255	4.2	237	7440.45[d,]
51282.90	+31	Lick 3m	KAST	3321-10483	3.2	46	5489.40[c]
51284.84	+33	ESO 3.6m	EFOSC	3392-10128	4.2	195	7363.23[d,]
51290.84	+39	ESO 3.6m	EFOSC	3344-10194	4.2	146	7435.50[d,]
51293.97	+42	Lick 3m	KAST	3268-8002	2.1	49	5417.33[c]

[a] Average wavelength-bin size.

[b] Average signal-to-noise ratio per wavelength bin.

[c] Beginning of red channel, [Å].

[d] Negligible 2nd order contamination.

[e] Possible 2nd order contamination above 7500 Å.

[f] Rest Frame.

Table 2: Synow parameters for -15 days. The fit is shown in Fig. 5. v_{phot}=13000 km s^{-1}, $T_{bb} = 11200$ K.

Ion	τ	v_{min} 10^3 kms^{-1}	v_{max} 10^3 kms^{-1}	T_{exc} 10^3K	v_e 10^3 kms^{-1}
C II	0.038	16	40	15	5
C III	0.2		14.2	15	5
O I	0.2	-	40	15	5
Mg II	0.15	-	40	15	5
Si II	0.65	14.2	40	15	5
Si III	0.42	-	17	15	5
S II	0.2	-	17	15	5
Ca II	1.5	16	40	15	5
Fe III	0.55	14.5	18	12	5
Co II	0.006	-	40	15	5
Ni III	5	-	40	12	5

Table 3: Synow parameters for −9 days. The fit is shown in Fig. 5. v_{phot}=11800 km s^{-1}, $T_{bb} = 13800$ K.

Ion	τ	v_{min}	v_{max}	T_{exc}	v_e
		10^3 kms^{-1}	10^3 kms^{-1}	10^3K	10^3 kms^{-1}
C II	0.015	16	40	12	5
C III	0.75		12.8	12	5
O I	0.1	-	40	12	5
Mg II	0.2	-	40	12	5
Si II	1.2	-	40	12	5
Si III	0.6	-	16	12	5
S II	0.2	-	17	12	5
Ca II	1.5	16	40	12	5
Fe III	0.65	-	18	12	5
Ni III	-	-	40	12	5
Co II	0.045	-	40	12	5